Increased drought resistance in state transition mutants is linked to modified plastoquinone pool redox state

Lucas Leverne, Thomas Roach, François Perreau, Fabienne Maignan, Anja Krieger-liszkay

Received: 17 March 2023 | Revised: 1 August 2023 | Accepted: 7 August 2023

DOI: 10.1111/pce.14695

ORIGINAL ARTICLE

Plant, Cell & Environment | WILEY

Increased drought resistance in state transition mutants is linked to modified plastoquinone pool redox state

Lucas Leverne[1] | Thomas Roach[2] | François Perreau[3] | Fabienne Maignan[4] | Anja Krieger-Liszkay[1]

[1]Institute for Integrative Biology of the Cell (I2BC), CEA, CNRS, Université Paris-Saclay, Gif-sur-Yvette, France

[2]Department of Botany, University of Innsbruck, Innsbruck, Austria

[3]INRAE, AgroParisTech, Institut Jean-Pierre Bourgin (IJPB), Université Paris-Saclay, Versailles, France

[4]Laboratoire des Sciences du Climat et de l'Environnement, LSCE/IPSL, CEA-CNRS-UVSQ, Université Paris-Saclay, Gif-sur-Yvette, France

Correspondence
Anja Krieger-Liszkay, Institute for Integrative Biology of the Cell (I2BC), CEA, CNRS, Université Paris-Saclay, 91198 Gif-sur-Yvette cedex, France.
Email: anja.liszkay@i2bc.paris-saclay.fr

Funding information
Agence Nationale de la Recherche; CLand ANR-16-CONV-0003; Saclay Plant Science; Labex Saclay Plant Sciences-SPS, Grant/Award Number: ANR-17-EUR-0007; French Infrastructure for Integrated Structural Biology, Grant/Award Number: ANR-10-INSB-05

Abstract

Identifying traits that exhibit improved drought resistance is highly important to cope with the challenges of predicted climate change. We investigated the response of state transition mutants to drought. Compared with the wild type, state transition mutants were less affected by drought. Photosynthetic parameters in leaves probed by chlorophyll fluorescence confirmed that mutants possess a more reduced plastoquinone (PQ) pool, as expected due to the absence of state transitions. Seedlings of the mutants showed an enhanced growth of the primary root and more lateral root formation. The photosystem II inhibitor 3-(3,4-dichlorophenyl)−1, 1-dimethylurea, leading to an oxidised PQ pool, inhibited primary root growth in wild type and mutants, while the cytochrome b_6f complex inhibitor 2,5-dibromo-3-methyl-6-isopropylbenzoquinone, leading to a reduced PQ pool, stimulated root growth. A more reduced state of the PQ pool was associated with a slight but significant increase in singlet oxygen production. Singlet oxygen may trigger a, yet unknown, signalling cascade promoting root growth. We propose that photosynthetic mutants with a deregulated ratio of photosystem II to photosystem I activity can provide a novel path for improving crop drought resistance.

KEYWORDS
photosynthesis, plastoquinone redox state, root growth, singlet oxygen, state transitions

1 | INTRODUCTION

Drought-resistant plants are required to cope with the increase in world population and the challenges of predicted climate change. New traits need to be identified and methods have to be developed to maintain and improve crop productivity under harsh environmental conditions. Water and nutrients are absorbed by plant roots and specific root traits, such as growth and architecture, are important under unfavourable conditions, e.g. drought. Previously it has been shown that inhibition of the carotenoid biosynthesis pathway reduces root growth and the emergence of lateral roots in *Arabidopsis thaliana*, demonstrating the importance of carotenoids for root growth (Van Norman et al., 2014). It has been shown that strigolactones and abscisic acid, both being phytohormones derived from carotenoids, regulate root growth and branching of lateral roots (Gomez-Roldan et al., 2008; Ruyter-Spira et al., 2011). Furthermore, the volatile β-cyclocitral that is either enzymatically produced by carotenoid cleavage dioxygenases or by the non-enzymatic

$^1O_2$–dependent oxidation of β-carotene has been found to be a root growth regulator (Dickinson et al., 2019). Beside β-cyclocitral, other carotenoid cleavage products (apocarotenoids) and reactive electrophile species (RES) may be capable of promoting root growth and development (Biswas et al., 2019).

Apocarotenoids are generated either by non-enzymatic or enzymatic carotenoid oxidation. Singlet oxygen ($^1O_2$) oxidises β-carotene to, amongst others, β-cyclocitral or β-ionone, both of which can influence plant growth and development. β-cyclocitral has been shown to induce drought resistance in *Arabidopsis thaliana* (D'Alessandro et al., 2019). In photosystem II (PSII) chlorophyll in its triplet state (^{3}Chl) reacts with oxygen, a triplet in its ground state, producing $^1O_2$. ^{3}Chl is generated by charge recombination reactions of the primary radical pair in PSII (Krieger-Liszkay, 2005; Rutherford and Krieger-Liszkay, 2001). Charge recombination leads to the formation of the primary radical pair P^+Ph^-, with pheophytin (Ph) being the primary electron acceptor in PSII, and subsequently to the repopulation of the excited state of P680. The excited state formed can be either a singlet or a triplet state (^{3}P680), depending on the charge recombination route. The probability of charge recombination within PSII increases when the plastoquinone (PQ) pool and the acceptor side of PSII are reduced, for example, when there is a lack of stromal electron acceptors under CO_2 limitation from drought-induced stomatal closure.

The redox state of the PQ pool is also influenced by movements of the light-harvesting antenna trimer (L-LHCII), which changes the absorption cross-sections of PSII and PSI in a process called state transition. Both phosphorylation (Bellafiore et al., 2005; Depège et al., 2003) and N-terminal acetylation (Koskela et al., 2018) are posttranslational modifications of proteins involved in this process. Phosphorylation and acetylation of L-LHCII are required to allow the detachment of L-LHCII from PSII to adjust the amount of excitation energy received by the two photosystems (Koskela et al., 2018). These posttranslational modifications are highly dynamic and are often regulated by changes in the environment and stress (e.g., Linster & Wirtz, 2018; Stone & Walker, 1995). When more light is absorbed by PSII than by PSI, L-LHCII attached to PSII becomes phosphorylated and acetylated. The modified L-LHCII detaches from PSII and migrates to PSI, thereby increasing the cross-section and excitation of PSI. Lysine acetylation of L-LHCII is achieved by the chloroplast acetyltransferase enzyme *NSI* (NUCLEAR SHUTTLE INTERACTING; At1G32070) (Koskela et al., 2018). The reduction of the PQ pool regulates the activity of the serine/threonine-protein kinase STN7 (Bellafiore et al., 2005; Depège et al., 2003), while an oxidised PQ pool leads to dephosphorylation of LHCII by the phosphatase PPH1/TAP38 (Pribil et al., 2010; Shapiguzov et al., 2010). N-terminal acetylation has been shown to decrease significantly after drought stress, and transgenic downregulation of this activity induced drought tolerance (Linster et al., 2015). How state transitions are linked to drought tolerance remains unclear.

We hypothesise that a higher reduction state of the PQ pool and concomitant $^1O_2$ generation leads to a signalling event that induces drought stress tolerance. To test this, we investigated drought resistance in *Arabidopsis thaliana*, using the well-characterised state transition mutant *stn7*, and the less well-characterised mutants, *nsi1* and *nsi2*, two knockout lines lacking the chloroplast acetyltransferase *NSI*.

2 | MATERIALS AND METHODS

2.1 | Plant material and plant growth conditions

Arabidopsis thaliana (ecotype Columbia-0) wild type (WT) *stn7*, *nsi1*, and *nsi2* were grown in Jiffy-7®—Peat Pellets in plastic pots (5 cm high, 5.5 cm diameter) in ambient air for 4 weeks in a growth cabinet in long-day conditions: 16 h of light (22°C), 8 h of dark (18°C), and at a light intensity of 110 µmol quanta m^{-2} s^{-1} (light source, fluorescent light tubes; OSRAM fluora 58 Watt/77). To achieve mild drought stress, watering was stopped for 4–6 days. For each replicate, plants in control and stress conditions of the same age were used.

2.2 | Seedling growth conditions

WT, *stn7*, *nsi1*, and *nsi2* seeds were sterilised in a solution of ethanol 70% (vol/vol) and sodium dodecyl sulfate 0.05% (wt/vol) under gentle agitation for 12 min, washed three times with ethanol 96%, and then dried on a sterile filter paper. Seeds were grown in one-half-strength Gamborg's B5 agar medium (Gamborg et al., 1968). Seeds were stratified in the dark at 4°C for 48 h. Then plates were placed in a growth cabinet 16/8 h day/night, at 22°C/18°C, fluorescent light 110 µmol quanta m^{-2} s^{-1}. Supplements including 3-(3,4-dichlorophenyl)−1,1-dimethylurea (DCMU, 2 µM), 2,5-dibromo-3-methyl-6-isopropylbenzoquinone (DBMIB, 30 µM), and mannitol (200 mM) were added directly to the agar medium. The stability of DBMIB in the light was tested by measuring the inhibitory effect of the DBMIB solution after 10 days of storage in the growth cabinet under the same photoperiod and temperature as above. Photosynthetic electron transport activity of thylakoids was still inhibited by 80% in the presence of 3 µM DBMIB. In seedlings, when grown in the presence of 2 µM DCMU, Fv/Fm was low (0.355 ± 0.015) and Y(II) close to zero at low light intensity (21 µmol quanta m^{-2} s^{-1}). When grown in the presence of DBMIB, Fv/Fm was lower than without herbicide (0.59 ± 0.09), Y(II) was 0.277 at low light (21 µmol quanta m^{-2} s^{-1}). Without addition, Fv/Fm was 0.751 ± 0.01 and Y(II) 0.501 ± 0.005 (21 µmol quanta m^{-2} s^{-1}).

2.3 | Rosette size and relative water content (RWC)

Rosette size of the different genotypes was determined using pixel numbers of stationary fluorescence levels of fluorescence images taken by the Imaging-PAM. For the determination of RWC, total rosettes were sampled and weighed. Saturated weight was determined by weighing the rosettes after a 12 h immersion in water at 4°C in the dark. Dry weight was determined by weighing rosettes after drying for 48 h at 70°C. RWC was calculated using:

RWC = (FW − DW)/(SW − DW) where FW, SW, and DW are the rosette fresh, water-saturated, and dry weights, respectively.

2.4 | Stomata opening

To observe the stomata under the microscope, transparent tape was applied to the abaxial part of the leaf, and it was quickly torn off so that a thin layer of the lower epidermis could be removed and fixed to be observed under the microscope. The ratio of width/length was determined with an optical microscope ×40 (Zeiss Axio Imager M1), measured manually using the Fiji software, at least for 100 stomata for each condition and each genotype.

2.5 | Chlorophyll fluorescence

Chlorophyll fluorescence was measured on whole plants at room temperature with an Imaging-PAM Maxi-Version (Walz). Plants were adapted for 15 min in the dark before measuring the minimum fluorescence level Fo. A saturating flash (300 ms, 10 000 µmol quanta $m^{-2}\,s^{-1}$) was given to determine the maximum fluorescence Fm. To measure the maximum fluorescence level in the light, Fm′, plants were illuminated for 3 min with different intensities of actinic light (55, 80, 110, 145, 185, 230, 335, 425, 610 µmol quanta $m^{-2}\,s^{-1}$), and a saturating flash was given at the end of each light intensity step.

Parameters are defined as follows: F: fluorescence yield; F_0': dark fluorescence level after illumination; Fm′: maximal fluorescence yield in the light; NPQ: nonphotochemical fluorescence quenching; Y(II): effective PSII quantum yield; Y(NPQ): quantum yield of regulated energy dissipation in PSII; Y(NO): quantum yield of nonregulated energy dissipation in PSII; qP: photochemical quenching; qL: fraction of open PSII reaction centres. The different fluorescence parameters are calculated as follows: Y(II) = (Fm′ − F)/Fm′; NPQ = (Fm − Fm′)/Fm′; Y(NPQ) = 1 − Y(II) − 1/(NPQ + 1 + qL(Fm/Fo-1)); Y(NO) = 1/(NPQ + 1+ qL(Fm/Fo − 1)); qP = (Fm′ − F)/(Fm′ − Fo′); qL = qP × Fo′/F.

2.6 | 77K chlorophyll fluorescence measurements

Fluorescence emission spectra of isolated thylakoids were measured with a Carry Eclipse fluorimeter; excitation wavelength: 430 nm; monochromator slits: 5 nm; scanning speed: 120 nm min^{-1}; averaging time: 0.5 s; average of 6 scans. The intensities were normalised to the intensity of the PSII emission.

2.7 | Spin-trapping electron paramagnetic resonance (EPR) spectroscopy

$^1O_2$ was trapped using the water-soluble spin probe 2,2,6,6-tetramethyl-4-piperidone hydrochloride (TEMPD-HCl) (Hideg et al., 2011). Thylakoids from Arabidopsis were prepared using a standard protocol (e.g., Messant et al., 2018). Thylakoids (20 µg chlorophyll mL^{-1}) were illuminated for 2 min with red light (Schott filter RG 630) at 670 µmol quanta $m^{-2}\,s^{-1}$ in 100 mM TEMPD-HCl, 0.3 M sorbitol, 50 mM KCl, 1 mM $MgCl_2$ and 25 mM HEPES (pH 7.6). Spin-trapping assays for detecting $^{\bullet}OH$ derived from $O_2^{\bullet-}/H_2O_2$ were carried out using the spin trap 4-pyridyl1-oxide-N-tert-butylnitrone (4-POBN). Leaves were vacuum-infiltrated with a buffer (25 mM HEPES, pH 7.5, 5 mM $MgCl_2$, 0.3 M sorbitol) containing the spin trap reagents (50 mM 4-POBN, 4% ethanol, 50 µM Fe-EDTA). Infiltrated leaves were placed into the buffer containing the spin trap reagents and illuminated for 30 min with white light (100 µmol quanta $m^{-2}\,s^{-1}$). At the end of the illumination time, the leaves were removed and the EPR signal of the solution was monitored. EPR spectra were recorded at room temperature in a standard quartz flat cell using an ESP-300 X-band spectrometer (Bruker). The following parameters were used: microwave frequency 9.73 GHz, modulation frequency 100 kHz, modulation amplitude: 1 G.

2.8 | Analysis of aldehydes, including RES and β-cyclocitral, with LC-MS/MS

Aldehydes were measured according to Roach et al. (2017). Briefly, leaves frozen in liquid nitrogen were ground for 1 min inside 2 mL reaction tubes using 2 × 5 mm quartz beads in 1 mL of pre-cooled (−20°C) acetonitrile, containing 0.5 µM 2-ethylhexanal (as internal standard) and 0.05% (wt:vol) of butylated hydroxytoluene. The resulting extract was centrifuged for 10 min, 4°C, at 26 000*g*, and the supernatant was split with 600 µL used for the analysis of aldehydes and 200 µL for the measurement of chlorophyll. Aldehydes were derivatized with 2,4-Dinitrophenylhydrazine (2,4-DNPH) in the presence of formic acid and diluted 50:50 with LC-MS-grade H_2O before injection of 3 µL sample. Separation was carried out using a reversed-phase column (NUCLEODUR C18 Pyramid, EC 50/2, 50 × 2 mm, 1.8 µm, Macherey-Nagel), using an ekspert ultraLC 100 UHPLC system coupled to a QTRAP 4500 mass spectrometer (AB SCIEX). Peak areas of selected ions were normalised to 2-ethylhexanal and chlorophyll content of the sample. Chlorophyll was quantified by absorbance in 80% acetone using the extinction coefficients of Porra et al. (1989).

2.9 | Pigment analysis

Mature leaves were frozen in liquid nitrogen, lyophilised and ground. Powder (2 mg dry weight) was dissolved in 500 µL acetone, 0.01% ammoniac, then centrifugation at 12 000*g* 5 min, supernatants were collected and pellet washed twice in acetone. Solvent was evaporated and the precipitates were resuspended in 100 µL acetone. Liquid chromatography-UV-absorption (HPLC-UV) analysis was performed using a HPLC column (Uptisphere Strategy C18-HQ 250 × 3 mm, 3 µm granulometry, Interchim) with a HPLC/UV chain (Shimadzu) including two pumps (LC-20AD), a sample manager

(SIL-20AC HT), a column oven (CTO-20A) and an UV diode array detector (UVSPD-M20A) with a flow of 0.5 mL min^{-1}. The mobile phase A was composed of 10% water and 89.5% acetonitrile with 0.5% acetic acid and the mobile phase B was ethyl acetate with 0.5% acetic acid. The elution gradient was as follows: initially 10% B, 1 min 10% B; then a linear increase up to 95% B for 24 min. At the end, the column was returned to initial conditions for a 15 min equilibration. Absorbance was monitored at 450 nm. Signals were calculated by normalisation of peak areas to chlorophyll *a*.

2.10 | Enzyme activities

Crude protein extracts were prepared by grinding leaves in liquid nitrogen before adding a buffer containing 0.3 M sorbitol, 50 mM KCl, 5 mM $MgCl_2$, 20 mM HEPES pH 7.2. The supernatant after centrifugation (13 000*g*, 5 min, 4°C) was used for the measurements. Protein content was determined using Amioblack. Superoxide dismutase (SOD) activity was measured spectrophotometrically using xanthine/xanthine oxidase as superoxide generating system and XTT (Na,3′-(1-(phenylaminocarbonyl)−3,4-tetrazolium)-bis-(4-methoxy-6-nitro) benzene sulfonic acid hydrate) for the detection of superoxide. A stock solution of xanthine (500 µM) was freshly prepared in water, adding 1 M NaOH until it dissolved. The final assay contained 50 µM xanthine, 100 µM XTT and 0.2 U mL^{-1} xanthine oxidase in 20 mM HEPES pH 7.0. The kinetics of superoxide production were measured as an increase in absorbance at 470 nm, and the SOD activity was determined by following the inhibition of the superoxide production after addition of 10 µg protein mL^{-1} of crude extract. Superoxide production was calculated using the molar extinction coefficient $\varepsilon_{470} = 24.2\ mMl^{-1}\ cm^{-1}$ for XTT. Catalase activity was measured polarographically at 20°C with a Clark-type electrode in 50 mM HEPES (pH 8) in the presence of 1 mM H_2O_2 as substrate using a final protein concentration of 20 µg mL^{-1}. Guaiacol peroxidase activity was determined spectrophotometrically by measuring the oxidation of guaiacol to tetraguaiacol at 470 nm. At this wavelength, the molar extinction coefficient of tetraguaiacol is 26.6 $mM^{-1}\ cm^{-1}$. The reaction mixture contained 50 mM NaH_2PO_4/Na_2HPO_4 pH 7.5, 3 mM H_2O_2 and 0.01% (vol/vol) guaiacol, and 10 µg mL^{-1} protein.

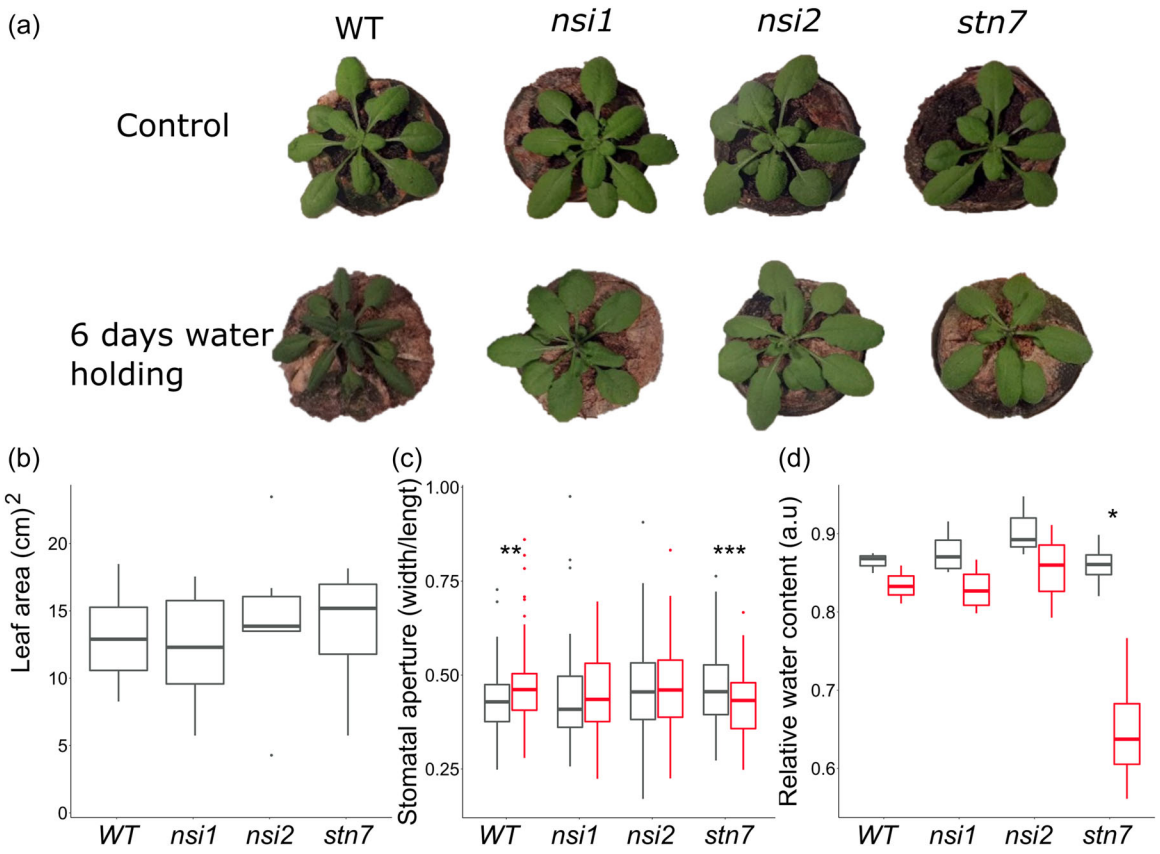

FIGURE 1 State transition mutants are more resistant to drought. (a) 4-week-old *A. thaliana* wild type and *nsi1*, *nsi2*, *stn7* plants well-watered and after 6 days without watering. (b) Rosette size ($n \geq 5$); plants from three different growth series. (c, d) Relative water content of total rosette in control conditions (grey) and after 4 days without watering (red). (d) Stomata aperture. Ratio width/length of stomata aperture in control conditions (black) and after 4 days without watering (red), counting about 100 stomata on at least three different leaves in each condition. Three replicates from four different independently grown sets of plants, $n = 12$, mean and *SD* are given. Stars indicate significant differences according to Student's *t* test (*$p < 0.05$, **$p < 0.01$, ***$p < 0.001$).

2.11 | Statistical analysis

Graphs and statistical tests were produced using the R software. For all boxplots, the various elements are defined as follows: upper whisker = largest observation less than or equal to upper hinge + 1.5 × inter-quartile range (IQR); lower whisker = smallest observation greater than or equal to lower hinge − 1.5 × IQR; centre line = median, 50% quantile; upper hinge = 75% quantile; lower hinge = 25% quantile; outliers are data beyond the end of the whiskers and represented by a dot; each dot in the box represents a single data point. Symbols represent the *p* value of Student test *: $p < 0.05$; **: $p < 0.01$; ***: $p < 0.001$; ****: $p < 0.0001$; no stars: $p > 0.05$.

3 | RESULTS

To investigate the drought stress tolerance of state transition mutants, we subjected wild type, *nsi1*, *nsi2*, and *stn7* to drought stress by withholding water for 6 days. The wild type leaves wilted while the state transition mutants were visibly much less affected (Figure 1a). The rosette sizes of the different genotypes were similar in well-watered plants (Figure 1b). For the following experiments water was withhold for 4 days to induce moderate drought stress. Under this condition, photosynthetic electron transport is not considered the primary damage site (Cornic & Fresneau, 2002; Kaiser, 1987). Upon moderate drought stress, the rosettes of the mutants showed a much higher water content (Figure 1c). Furthermore, stomata were significantly more closed in wild type upon moderate drought stress, while there was no change in stomata opening in the mutants (Figure 1d).

Since the mutants are affected in their ability to adapt the antenna size dependent on the light quality, intensity, and stress conditions, we investigated the effect of moderate drought on photosynthesis. No significant differences in chlorophyll and carotenoid compositions were observed between the genotypes with or without drought stress (SI Table 1). Upon drought, the content of β-carotene, lutein and neoxanthin increased in all genotypes. Analysis of chlorophyll fluorescence parameters showed that upon drought the effective quantum yield of photosystem II (YII) was significantly affected in wild type while there were no significant changes in the mutants (Figure 2a). For the statistical analysis, values measured at a light intensity of 100 µmol quanta m^{-2} s^{-1} were chosen, an intensity close to the growth light intensity. When the light intensity exceeds the optimal intensity for assimilation, energy dissipation at the level of PSII sets in. According to Kramer et al. (2004), two types of quantum yields for energy dissipation can be defined, Y(NPQ) and Y (NO) which represent regulated and non-regulated energy dissipation, respectively. Dissipation of excess energy expressed as the yield of non-photochemical quenching, Y(NPQ), increased significantly in the wild type upon drought while it remained constant in the mutants

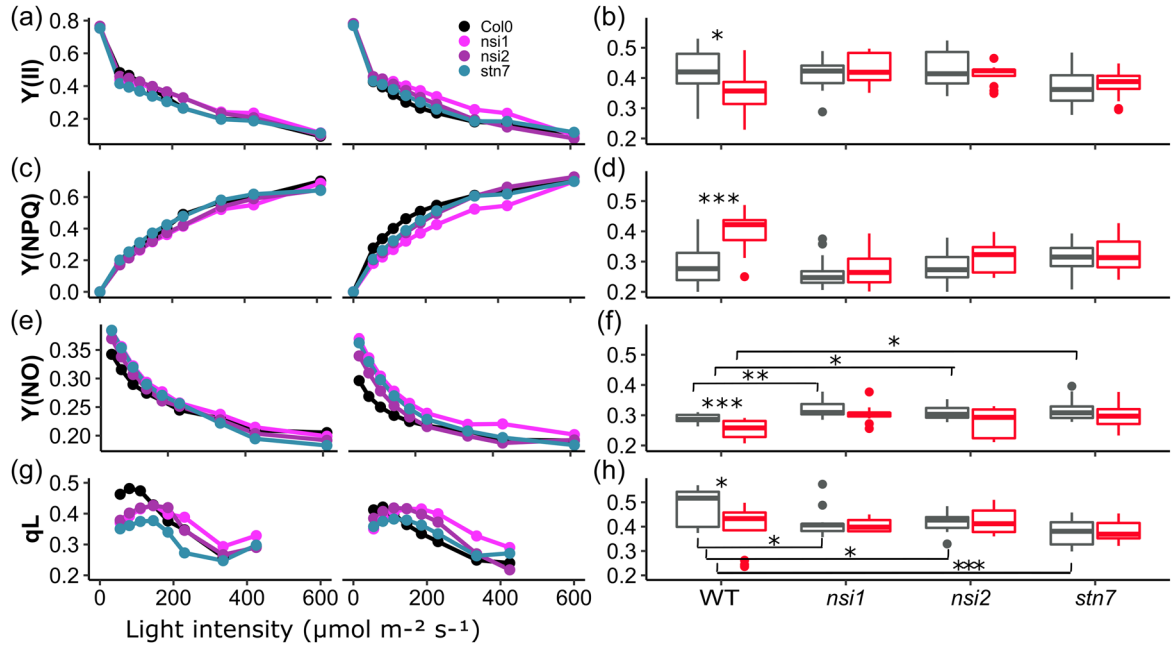

FIGURE 2 State transition mutants show no changes in the light dependency of chlorophyll fluorescence parameters upon moderate drought stress. Left: light response curves of fluorescence parameters in control conditions or after 4 days without watering (stress). (a, b) effective quantum yield PSII, Y(II), (c, d) controlled non-photochemical quenching, Y(NPQ), (e, f) Non-regulated non-photochemical quenching, Y(NO), and (g, h) fraction of open PSII centres, qL. The left panel shows variations of the fluorescence parameters as a function of the light intensity; the right panel shows boxplots of the fluorescence parameters for wild type and *nsi1*, *nsi2*, *stn7* at growth light intensity (100 µmol m^{-2} s^{-1}). Each light intensity was applied for 3 min before giving a saturating light flash. Three replicates from four different independently grown sets of plants, $n = 12$, mean and *SD* are given. Stars indicate significant differences according to Student's *t* test (*$p < 0.05$, **$p < 0.01$, ***$p < 0.001$).

(Figure 2b). Relevant here is that state transitions have only a minor contribution to chlorophyll fluorescence measurements of Y(NPQ), thus lack of change of Y(NPQ) in the mutants reflects lack of stress. This was the case of the regulated part of NPQ while the non-regulated quenching, Y(NO), decreased in the wild type upon stress (Figure 2c). When the genotypes were compared in control conditions, Y(NO) was significantly higher in the mutants, showing that state transitions influence chlorophyll fluorescence at growth light intensity. The larger amount of LHCII at PSII has the consequence that reaction centres of PSII were more closed in the mutants as indicated by significantly lower qL values in the control conditions, i.e., the primary quinone acceptor Q_A accumulated more in its reduced form in the mutants. In the case of qL, there was a significant decrease in the wild type upon drought, showing that more reaction centres were closed, while no significant differences were observed for the mutants (Figure 2h).

The results of the chlorophyll fluorescence parameters are in line with a lack of state transition in the mutants, however, they do not

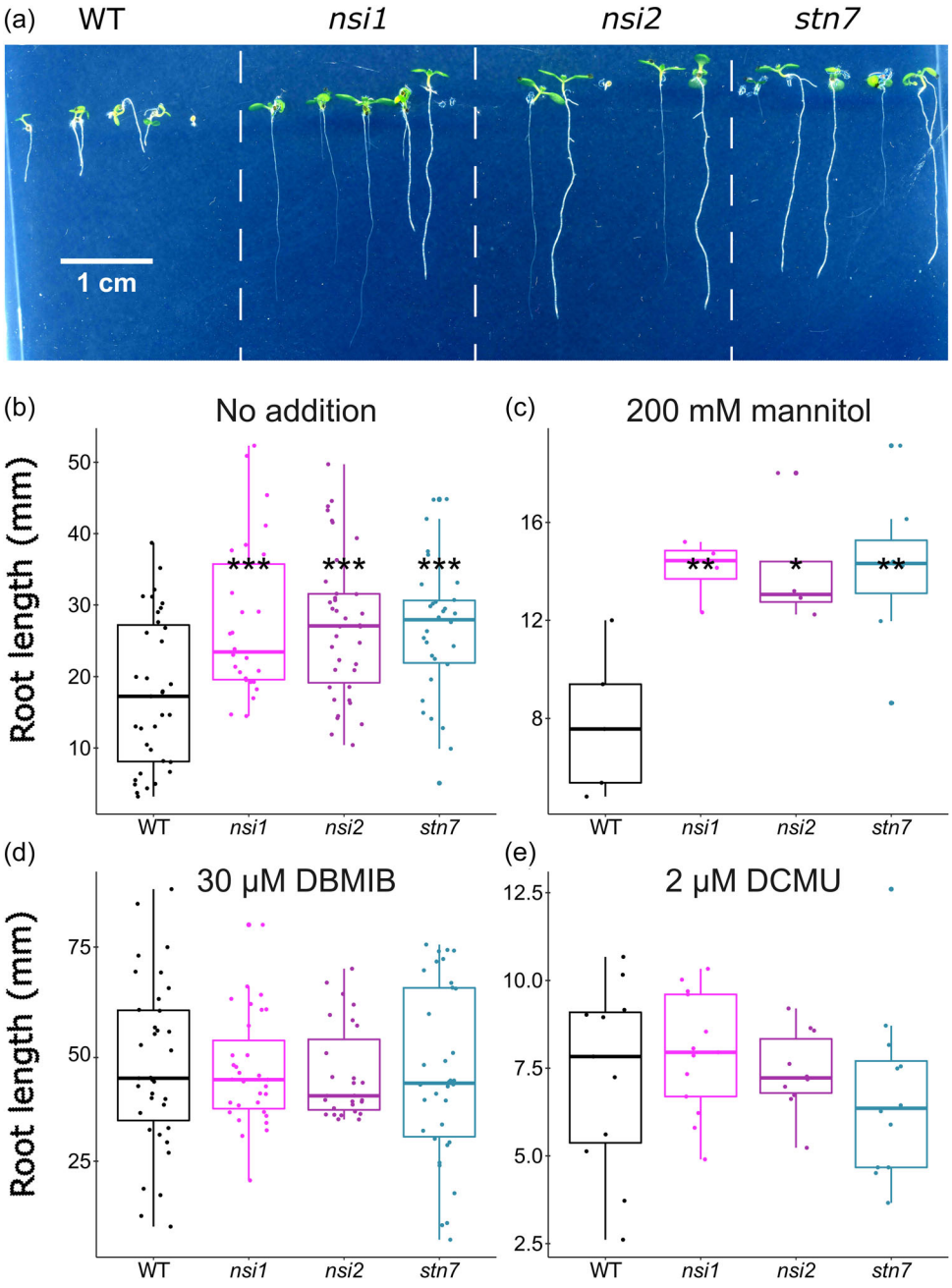

FIGURE 3 State transitions mutants show stimulation of growth root. (a) Photos of seedings of WT, *nsi1*, *nsi2*, and *stn7* after 7 days. (b) Length of the primary root of 7 days old in control conditions, $n \geq 21$. (c) Length of the primary root of 7 days old in the presence of 200 mM mannitol. (d, e) Length of the primary root of 7 days old in the presence of 30 µM DBMIB, $n \geq 10$, and 2 µM DCMU respectively, $n \geq 10$. Mean and *SD* are given. Stars indicate significant differences according to Student's *t* test (*$p < 0.05$, **$p < 0.01$).

explain their improved drought tolerance. Since it has been described previously that N-acetylation of protein is important for germination and root development (Linster et al., 2015), we investigated the root growth of the seedlings. As shown in Figure 3a,b, the main root of the wild type was thinner and shorter compared with the mutants. In addition, lateral root development was strongly enhanced in the mutants. Differences in root architecture between the genotypes were not only observed in seedlings but also in 4-week-old plants grown in soil, with the wild type showing a slightly less well-developed root system (Figure S1). The difference between the lengths of the main root in seedlings of wild type and mutants was even higher when plants were grown under osmotic stress conditions (200 mM mannitol) (Figure 3c). However, when the photosynthetic electron transfer was blocked by DCMU, an inhibitor that blocks electron transport in PSII by binding to the Q_B-site of the D1 protein, or by DBMIB, an inhibitor of the cytochrome b_6f complex that binds to the Qo-binding site, differences between the genotypes were no longer observed. In the presence of DBMIB that leads to a more reduced PQ pool, growth of the main root was even stimulated in all genotypes compared to control conditions, while growth was retarded in the presence of DCMU that leads to an oxidised PQ pool. These results indicate that the reduction state of the PQ pool controls root growth.

In excess light conditions, more light is absorbed by the antenna than can be used for the reduction of $NADP^+$, and the PQ pool becomes more reduced. This is the case in the state transition mutants as seen by the lower qL compared to the wild type (Figure 2g,h). When Q_A is reduced, charge recombination reactions within PSII do occur between Q_A^- and the oxidised primary donor $P680^+$. This reaction leads to the generation of $^1O_2$, a highly oxidising reactive oxygen species. For visualising $^1O_2$ generation in leaves, we first used the fluorophore Singlet Oxygen Sensor Green, but, using this approach, we were not able to quantify differences between the four genotypes. Instead, we used an EPR spin probing assay with TEMPD as a probe to detect $^1O_2$ (Hideg et al., 2011). The assay cannot be performed with leaves or intact chloroplasts, and we used isolated thylakoid membranes instead. In thylakoids from wild-type plants, the L-LHCII is partly localised at PSI as is the case in leaves, while in the mutants all LHCII is localised at PSII as shown by 77K fluorescence (Figure 4a). As expected, when the PQ pool is more oxidised, less $^1O_2$ was generated in wild type compared with the mutants (Figure 4b,c).

To investigate whether there is a general increase in ROS generation in state transition mutants, we measured $O_2^{\bullet-}/H_2O_2$-derived hydroxyl radicals by a spin-trapping assay with 4-POBN/EtOH as a trap (Mubarakshina et al., 2010). Furthermore, the activity of a few antioxidant enzymes was measured. The amounts of $O_2^{\bullet-}/H_2O_2$ and the activities of the antioxidant enzymes superoxide dismutase, peroxidase, and catalase were slightly enhanced only in the wild type upon drought stress with only changes in peroxidase activity being statistically significant (Figure S2). In the mutants, the activities were unaltered or decreased upon drought in most cases. A statistically significant decrease of peroxidase activity was observed in *stn7*. However, an increase in catalase activity was observed in *nsi2*, although this increase was not significant. These data show that there was not a general increase in the level of oxidative stress in the mutants, but instead, a specific rise of $^1O_2$ levels. In the PSII reaction centre, $^1O_2$ can react with β-carotene, leading to oxidation products like β-cyclocitral and β-ionone. In addition, $^1O_2$ can react with lipids giving rise to additional RES. Figure 5 shows the most abundant RES detected in leaves from the wild type and the state transition

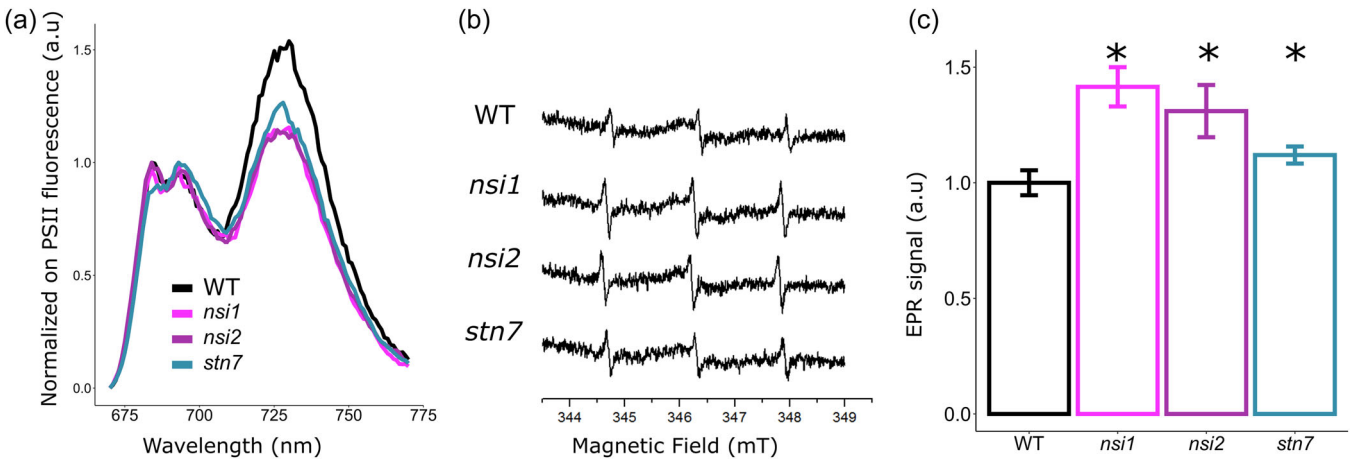

FIGURE 4 Thylakoid membranes of state transition mutants generate more singlet oxygen. (a) 77K chlorophyll fluorescence emission spectra of isolated thylakoid membranes. Signal normalised to PSII emission at 695 nm. Representative spectra are shown ($n = 3$). When chlorophyll *a* fluorescence emission spectra are measured at 77K, there are three emission maxima, two arising from PSII at 685 and 695 nm wavelength, and one arising from PSI around 733 nm wavelength. The lower emission from PSI in the mutants demonstrates that state transitions are not functional, and all LHCII are bound to PSII. (b) Detection of singlet oxygen by EPR using the spin probe TEMPD-HCl. Typical spectra are shown. (c) Quantification of the EPR signals ($n = 4$, 2 thylakoid preparations from set of plants grown at different times). (c) Quantification of the EPR signals shown in (b). Mean and *SD* are given. Stars indicate significant differences according to Student's *t* test ($^*p < 0.05$).

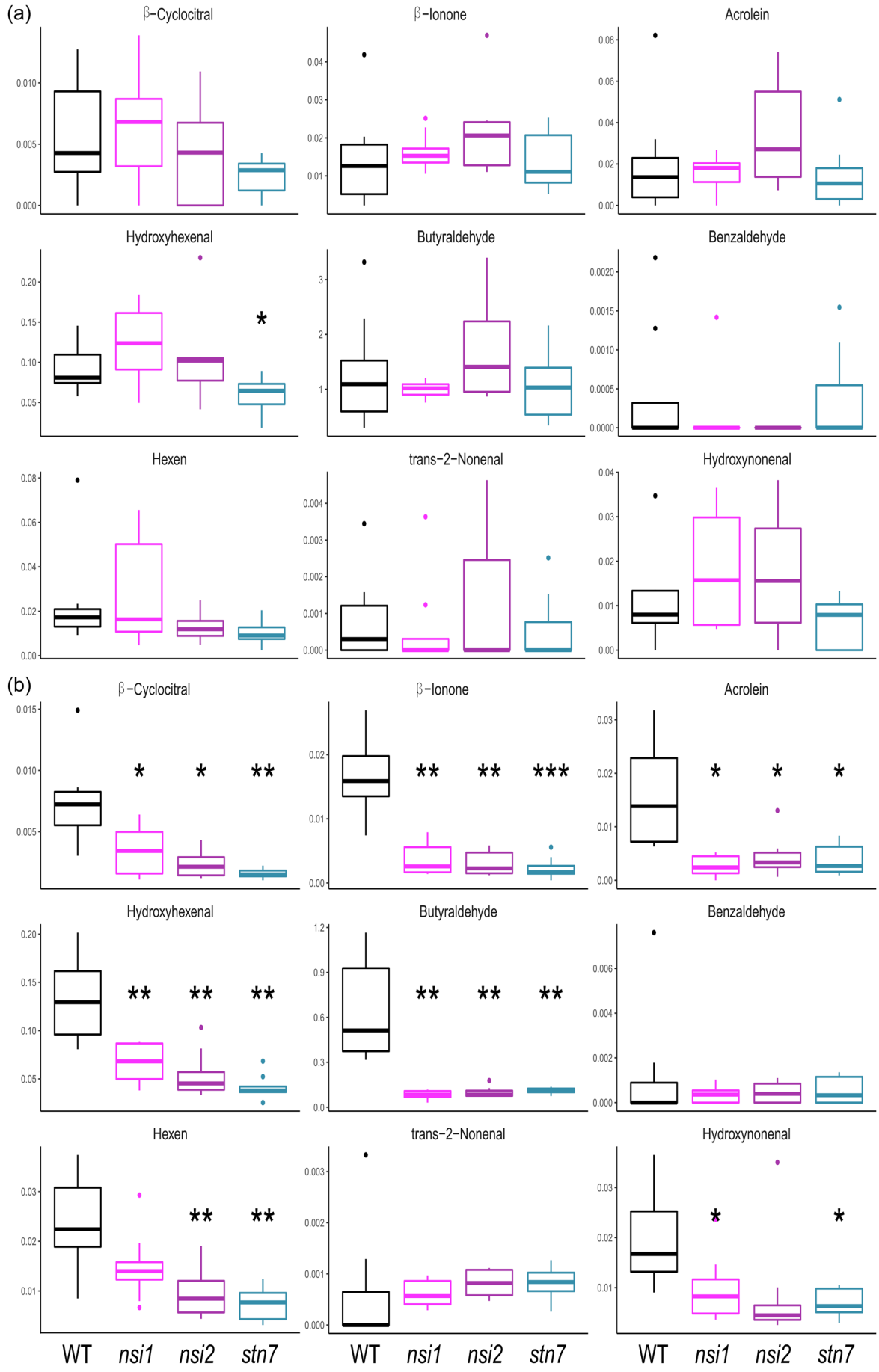

FIGURE 5 (See caption on next page).

mutants. In control conditions, there is no significant difference between the genotypes (Figure 5a), while upon moderate drought stress the wild type generated significantly more β-cyclocitral, β-ionone, acrolein, hydroxyhexanal, and butyraldehyde (Figure 5b). This is typical for a plant submitted to stress conditions. This shows that the wild-type plants are highly stressed, as already visible by the eye, while the state transition mutants cope with moderate drought stress without showing stress symptoms (Figure 1a).

4 | DISCUSSION

State transitions are controlled by the reduction state of the PQ pool via the activation of the STN7 kinase (Bellafiore et al., 2005; Depège et al., 2003). The results reported here raise the question of how the reduction state of the PQ pool affects root development. According to the data shown in Figure 3, the reduction state of the plastoquinone pool is crucial for primary root growth and lateral root development. In state transition mutants, the PQ pool is more reduced than in the wild type (Figure 2h). In all genotypes, when the PQ pool is reduced in the presence of DBMIB, root growth is stimulated (Figure 3d), whereas shorter roots are observed when the PQ pool is oxidised in the presence of DCMU (Figure 3e). Both, DCMU and DBMIB, inhibit photosynthetic electron transport, thereby showing that it is indeed the redox state of the PQ pool that exerts control of root growth and not differences in photosynthesis and sugar production. The inhibitory effect of DCMU on primary and lateral root growth has been observed previously and has been interpreted as photosynthesis promoting lateral root emergence partly through auxin biosynthesis (Duan et al., 2021). A yet unknown link between the redox state of the PQ pool and auxin signalling may be responsible for the observed differences in root architecture.

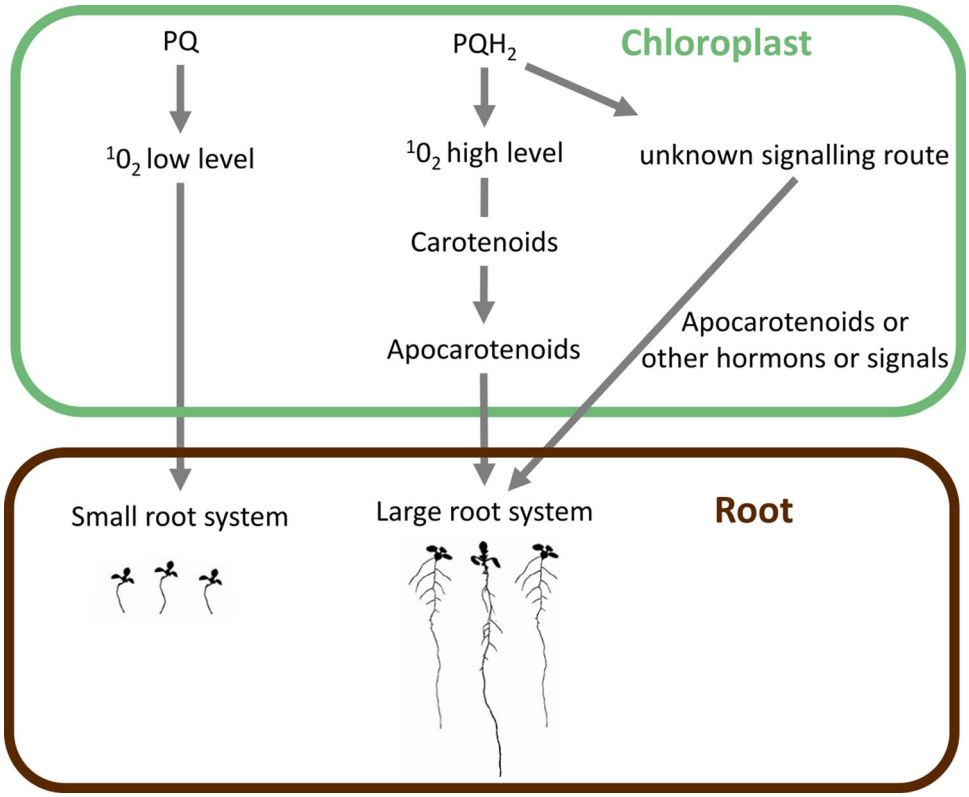

FIGURE 6 Connection between chloroplast redox state/$^1O_2$ generation and a long distance signalling pathway. When LHCII is blocked in state I (*stn7*, *nsi1*, *nsi2*), the plastoquinone pool is highly reduced in growth light in well-watered conditions. A highly reduced plastoquinone pool favours $^1O_2$ generation within PSII via charge recombination reactions between the primary donor P680 and the primary quinone acceptor Q_A^-. $^1O_2$ is supposed to react with β-carotene inside the reaction centre giving rise to the formation of apocarotenoids like β-cyclocitral. Its oxidation product, β-cyclocitric acid, is water soluble and could be transported from the shoot to the root, initiating signalling events far from the site of production. Other signalling events depending on the reduction state of the PQ pool are also imaginable.

FIGURE 5 Generation of reactive electrophile species is stimulated in wild type upon moderate drought stress. (a) Amounts of RES in leaves of 4-week-old WT, *nsi1*, *nsi2*, and *stn7* in control conditions. Shown are ion peak areas relative to the internal standard and normalised to the chlorophyll content of the extract. (b) Same as (a) after 4 days without watering ($n = 8$, independently grown sets of plants). Mean and *SD* are given. Stars indicate significant differences according to Student's *t* test (*$p < 0.05$, **$p < 0.01$, ***$p < 0.001$). WT, wild type.

As shown in Figure 4, state transition mutants generate slightly more $^1O_2$ than the wild type. $^1O_2$ may be the key to signalling events that promote root growth. Addition of DCMU inhibited root growth (Figure 3e), speaking at a first glance against the hypothesis that $^1O_2$ is responsible for the stimulation of root growth. However, although the addition of DCMU favours charge recombination in PSII, the yield of $^1O_2$ is low thanks to the modification of the midpoint potential of the redox couple Q_A/Q_A^- favoring charge recombination between $P680^+$ and Q_A^- via a direct route that does not yield ^{3}Chl (Fufezan et al., 2002; Krieger-Liszkay & Rutherford, 1998). The redox state of the PQ pool is known to be important for retrograde signalling (Dietz et al., 2016; Pfalz et al., 2012). In retrograde signalling, a signal travels from the chloroplast to the nucleus within the same cell. Here, a signal is required that travels over long distances. Figure 6 illustrates the hypothetical signal pathway. $^1O_2$ may produce signals such as apocarotenoids that are able to initiate signalling events far from the site of their production. β-Carotene oxidation products such as the volatile β-cyclocitral and its direct water-soluble oxidation product, β-cyclocitric acid, are known to regulate nuclear gene expression through several signalling pathways (D'Alessandro et al., 2019; Ramel et al., 2012; Shumbe et al., 2017). However, we were not able to detect an increase in β-cyclocitral or other RES in leaves of state transition mutants compared to wild type in plants under control conditions. This may be because the difference in $^1O_2$ production was, although significant, small. Even smaller differences are expected in the subsequently generated β-carotene oxidation products. We may technically not be able to detect such small differences in RES. Differences in levels of β-cyclocitral or other RES may also depend on the developmental stage of the plants. The RES measurements were performed with mature leaves while the root phenotype was observed in young seedlings. Besides $^1O_2$ and RES, the redox state of the PQ pool may activate other signalling pathways that involve microRNAs (Bertolotti et al., 2021) or changes in hormone levels like abscisic acid and strigolactones favoring root growth (Gomez-Roldan et al., 2008; Ruyter-Spira et al., 2011).

In conclusion, alterations in state transition appear to be a promising trait for improving plant growth and thereby crop productivity under harsh environmental conditions. The signalling pathway has to be elucidated in future work. It should be explored whether other photosynthetic mutants which exhibit an imbalance between PSII and PSI activity are also more drought resistant. Mutants affected not only in the antenna systems but also in the activity of the photosystems seem to be promising avenue for exploring drought tolerance. Especially mutants with slight defects in the turnover of the cytochrome b_6f complex or in photosystem I may be of interest since their PQ pool is in a more reduced state. Mutants lacking small subunits, for example PsaI (Schöttler et al., 2017), or expressing only one isoform of certain subunits, for example PsaE1 or PsaE2 (Hald et al., 2008; Krieger-Liszkay et al., 2020), which do not show a strong phenotype in control conditions seem to be ideal candidates to test their resistance to drought stress.

ACKNOWLEDGEMENTS

We would like to thank Sandrine Cot (I2BC) for technical assistance and Paula Mulo (University of Turku, Finland) for sending us the seeds of the state transition mutants. This work was supported by the Labex Saclay Plant Sciences-SPS (ANR-17-EUR-0007), the platform of Biophysics of the I2BC supported by the French Infrastructure for Integrated Structural Biology (FRISBI; grant number ANR-10-INSB-05), this work has benefited from the support of IJPB's Plant Observatory technological platforms and this work benefited from the French state aid managed by the ANR under the "Investissements d'avenir" programme with the reference ANR-16-CONV-0003 (CLand). L.L. is supported by a CLand and SPS PhD fellowship.

DATA AVAILABILITY STATEMENT

The data that support the findings of this study are available from the corresponding author upon reasonable request. Data will be made available on demand.

ORCID

Thomas Roach http://orcid.org/0000-0002-0259-0468
François Perreau http://orcid.org/0000-0001-7873-9866
Anja Krieger-Liszkay http://orcid.org/0000-0001-7141-4129

REFERENCES

Bellafiore, S., Barneche, F., Peltier, G. & Rochaix, J.-D. (2005) State transitions and light adaptation require chloroplast thylakoid protein kinase STN7. *Nature*, 433, 892–895.

Bertolotti, G., Scintu, D. & Dello Ioio, R. (2021) A small cog in a large wheel: crucial role of miRNAs in root apical meristem patterning. *Journal of Experimental Botany*, 72, 6755–6767.

Biswas, M.S., Fukaki, H., Mori, I.C., Nakahara, K. & Mano, J. (2019) Reactive oxygen species and reactive carbonyl species constitute a feed-forward loop in auxin signaling for lateral root formation. *The Plant Journal*, 100, 536–548.

Cornic, G. (2002) Photosynthetic carbon reduction and carbon oxidation cycles are the main electron sinks for photosystem II activity during a mild drought. *Annals of Botany*, 89, 887–894.

D'Alessandro, S., Mizokami, Y., Légeret, B. & Havaux, M. (2019) The apocarotenoid β-cyclocitric acid elicits drought tolerance in plants. *iScience*, 19, 461–473.

Depège, N., Bellafiore, S. & Rochaix, J.-D. (2003) Role of chloroplast protein kinase Stt7 in LHCII phosphorylation and state transition in Chlamydomonas. *Science*, 299, 1572–1575.

Dickinson, A.J., Lehner, K., Mi, J., Jia, K.P., Mijar, M., Dinneny, J. et al. (2019) β-Cyclocitral is a conserved root growth regulator. *Proceedings of the National Academy of Sciences*, 116, 10563–10567.

Dietz, K.J., Turkan, I. & Krieger-Liszkay, A. (2016) Redox- and reactive oxygen species-dependent signaling into and out of the photosynthesizing chloroplast. *Plant Physiology*, 171, 1541–1550.

Duan, L., Pérez-Ruiz, J.M., Cejudo, F.J. & Dinneny, J.R. (2021) Characterization of CYCLOPHILLIN38 shows that a photosynthesis-derived systemic signal controls lateral root emergence. *Plant Physiology*, 185, 503–518.

Fufezan, C., Rutherford, A.W. & Krieger-Liszkay, A. (2002) Singlet oxygen production in herbicide-treated photosystem II. *FEBS Letters*, 532, 407–410.

Gamborg, O.L., Miller, R.A., & Ojima, K. (1968) Nutrient requirements of suspension cultures of soybean root cells. *Experimental Cell Research*, 50, 151–158.

Gomez-Roldan, V., Fermas, S., Brewer, P.B., Puech-Pagès, V., Dun, E.A., Pillot, J.P. et al. (2008) Strigolactone inhibition of shoot branching. *Nature*, 455, 189–194.

Hald, S., Pribil, M., Leister, D., Gallois, P. & Johnson, G.N. (2008) Competition between linear and cyclic electron flow in plants deficient in photosystem I. *Biochimica et Biophysica Acta (BBA) - Bioenergetics*, 1777, 1173–1183.

Hideg, É., Deák, Z., Hakala-Yatkin, M., Karonen, M., Rutherford, A.W., Tyystjärvi, E. et al. (2011) Pure forms of the singlet oxygen sensors TEMP and TEMPD do not inhibit photosystem II. *Biochimica et Biophysica Acta (BBA) - Bioenergetics*, 1807, 1658–1661.

Kaiser, W.M. (1987) Effects of water deficit on photosynthetic capacity. *Physiologia Plantarum*, 71, 142–149.

Koskela, M.M., Brünje, A., Ivanauskaite, A., Grabsztunowicz, M., Lassowskat, I., Neumann, U. et al. (2018) Chloroplast acetyltransferase NSI is required for state transitions in *Arabidopsis thaliana*. *The Plant Cell*, 30, 1695–1709.

Kramer, D.M., Johnson, G., Kiirats, O. & Edwards, G.E. (2004) New fluorescence parameters for the determination of QA redox state and excitation energy fluxes. *Photosynthesis Research*, 79, 209–218.

Krieger-Liszkay, A. (2004) Singlet oxygen production in photosynthesis. *Journal of Experimental Botany*, 56, 337–346.

Krieger-Liszkay, A., & Rutherford, A.W. (1998) Influence of herbicide binding on the redox potential of the quinone acceptor in photosystem II: relevance to photodamage and phytotoxicity. *Biochemistry*, 37, 17339–17344.

Krieger-Liszkay, A., Shimakawa, G. & Sétif, P. (2020) Role of the two PsaE isoforms on O2 reduction at photosystem I in *Arabidopsis thaliana*. *Biochimica et Biophysica Acta (BBA) - Bioenergetics*, 1861, 148089.

Linster, E., Stephan, I., Bienvenut, W.V., Maple-Grødem, J., Myklebust, L.M., Huber, M. et al. (2015) Downregulation of N-terminal acetylation triggers ABA-mediated drought responses in arabidopsis. *Nature Communications*, 6, 7640.

Linster, E. & Wirtz, M. (2018) N-terminal acetylation: an essential protein modification emerges as an important regulator of stress responses. *Journal of Experimental Botany*, 69, 4555–4568.

Messant, M., Timm, S., Fantuzzi, A., Weckwerth, W., Bauwe, H., Rutherford, A.W. et al. (2018) Glycolate induces redox tuning of photosystem II in vivo: study of a photorespiration mutant. *Plant Physiology*, 177, 1277–1285.

Mubarakshina, M.M., Ivanov, B.N., Naydov, I.A., Hillier, W., Badger, M.R. & Krieger-Liszkay, A. (2010) Production and diffusion of chloroplastic H_2O_2 and its implication to signalling. *Journal of Experimental Botany*, 61, 3577–3587.

Van Norman, J.M., Zhang, J., Cazzonelli, C.I., Pogson, B.J., Harrison, P.J., Bugg, T.D.H. et al. (2014) Periodic root branching in arabidopsis requires synthesis of an uncharacterized carotenoid derivative. *Proceedings of the National Academy of Sciences*, 111, E1300–E1309.

Pfalz, J., Liebers, M., Hirth, M., Grübler, B., Holtzegel, U., Schröter, Y. et al. (2012) Environmental control of plant nuclear gene expression by chloroplast redox signals. *Frontiers in Plant Science*, 3, 257.

Porra, R.J., Thompson, W.A. & Kriedemann, P.E. (1989) Determination of accurate extinction coefficients and simultaneous equations for assaying chlorophylls a and b extracted with four different solvents: verification of the concentration of chlorophyll standards by atomic absorption spectroscopy. *Biochimica et Biophysica Acta (BBA) - Bioenergetics*, 975, 384–394.

Pribil, M., Pesaresi, P., Hertle, A., Barbato, R. & Leister, D. (2010) Role of plastid protein phosphatase TAP38 in LHCII dephosphorylation and thylakoid electron flow. *PLoS Biology*, 8, e1000288.

Ramel, F., Birtic, S., Ginies, C., Soubigou-Taconnat, L., Triantaphylides, C. & Havaux, M. (2012) Carotenoid oxidation products are stress signals that mediate gene responses to singlet oxygen in plants. *Proceedings National Academy of Sciences USA*, 109, 5535–5540.

Roach, T., Baur, T., Stöggl, W. & Krieger-Liszkay, A. (2017) *Chlamydomonas reinhardtii* responding to high light: a role for 2-propenal (acrolein). *Physiologia Plantarum*, 161, 75–87.

Rutherford, A.W. & Krieger-Liszkay, A. (2001) Herbicide-induced oxidative stress in photosystem II. *Trends in Biochemical Sciences*, 26, 648–653.

Ruyter-Spira, C., Kohlen, W., Charnikhova, T., van Zeijl, A., van Bezouwen, L., de Ruijter, N. et al. (2011) Physiological effects of the synthetic strigolactone analog GR24 on root system architecture in arabidopsis: another belowground role for strigolactones? *Plant Physiology*, 155, 721–734.

Schöttler, M.A., Thiele, W., Belkius, K., Bergner, S.V., Flügel, C., Wittenberg, G. et al. (2017) The plastid-encoded PsaI subunit stabilizes photosystem I during leaf senescence in tobacco. *Journal of Experimental Botany*, 68, 1137–1155.

Shapiguzov, A., Ingelsson, B., Samol, I., Andres, C., Kessler, F., Rochaix, J.-D. et al. (2010) The PPH1 phosphatase is specifically involved in LHCII dephosphorylation and state transitions in arabidopsis. *Proceedings of the National Academy of Sciences*, 107, 4782–4787.

Shumbe, L., D'Alessandro, S., Shao, N., Chevalier, A., Ksas, B., Bock, R. et al. (2017) METHYLENE BLUE SENSITIVITY 1 (MBS1) is required for acclimation of arabidopsis to singlet oxygen and acts downstream of β-cyclocitral. *Plant, Cell & Environment*, 40, 216–226.

Stone, J.M. & Walker, J.C. (1995) Plant protein kinase families and signal transduction. *Plant Physiology*, 108, 451–457.

SUPPORTING INFORMATION

Additional supporting information can be found online in the Supporting Information section at the end of this article.

How to cite this article: Leverne, L., Roach, T., Perreau, F., Maignan, F. & Krieger-Liszkay, A. (2023) Increased drought resistance in state transition mutants is linked to modified plastoquinone pool redox state. *Plant, Cell & Environment*, 1–11. https://doi.org/10.1111/pce.14695